Publication Date: 23 April 2025
Archs Sci. (2025) Volume 75, Issue 1 Pages 20-25, Paper ID 2025204.
https://doi.org/10.62227/as/75204

Computational Architecture of Developed Batteries through 2D Hybrid Metal Materials: A Promising Method to Future Sustainable Energy

Fatemeh Mollaamin[1,*]
[1]Department of Biomedical Engineering, Faculty of Engineering and Architecture, Kastamonu University, Kastamonu 37150, Turkey
Corresponding authors: (e-mail: fmollaamin@kastamonu.edu.tr).

Abstract In this work, alkali metals of rubidium and cesium are studied through doping in lithium, sodium or potassium ion batteries. A vast study on H-capture by "LiRb (GeO–SiO), LiCs(GeO–SiO), NaRb(GeO–SiO), NaCs(GeO–SiO), KRb(GeO–SiO), KCs(GeO–SiO) ", was carried out including using "DFT" computations at the "CAM–B3LYP–D3/6–311+G (d,p)" level of theory. The hypothesis of the hydrogen adsorption phenomenon was figured out by density distributions of "CDD, TDOS, LOL" for nanoclusters of "LiRb(GeO–SiO)–2H_2, LiCs(GeO–SiO)–2H_2, NaRb(GeO–SiO)–2H_2, NaCs(GeO–SiO)–2H_2, KRb(GeO–SiO)–2H_2, KCs(GeO–SiO)–2H_2". The oscillation in charge density amounts displays that the electronic densities were mainly placed in the edge of "adsorbate/adsorbent" atoms during the adsorption status. As the benefits of "lithium, sodium or potassium" over "Ge/Si" possess its higher electron and "hole motion", permitting "lithium, sodium or potassium" devices to operate at higher frequencies than "Ge/Si" devices. A small portion of "Rb or Cs" entered the "Ge–Si" layer to replace the Li, Na or K sites might improve the structural stability of the electrode material at high multiplicity, thereby improving the capacity retention rate. Among these, potassium-ion batteries seem to show the most promise in terms of "Rb or Cs" doping.

Index Terms energy storage, alkali metal-ion battery, density of states, charge distribution, materials modeling, hydrogen adsorption

I. Introduction

Sodium/potassium-ion can be the prime chemistry replacement candidate for LIBs [1]–[6]. The potassium-ion has certain privileges over analogous lithium-ion like the cell design is plain, and both the material and the construction methods are cheaper. The major benefit is the high amount and low cost of potassium in evaluation with lithium, which makes potassium batteries an engaged replacement for large scale batteries like household energy-saving and electric devices. Another privilege of a potassium-ion battery over a lithium-ion battery is potentially charging in a short time [7]–[13].

Lately, "Si-, Ge- or Sn-carbide nanostructures" have been proposed as occupied "H-grabbing" compounds [14]–[16]. Whereas the polarizability of Si is more than C atom, it is assumed that "Si–C/Si nanosheet" might append to compositions more strongly in comparison to the pure C-nanostructures [17]–[19]. The previous investigations of energy-saving devices through H-adsorption have been tailored owing to "DFT calculations" with a semiconductor group of "Si/Ge/Sn/Pb nano-carbides" [20], "Mg-Al nanoalloy" [21] and "Al/C/ Si doping of BN nanocomposite" [22].

Nanomaterials with notable structures detect undertaking demands in the field of electrocatalysis, fuel cells, and energy-saving. Furthermore, "rubidium and cesium ions" are studied as electrolyte additives for "sodium-ion batteries". It is shown that adding small amount of "Rb^+ and Cs^+" into the electrolyte significantly modifies the chemical composition of solid electrolyte interphase on hard carbon surfaces, which results in a significant increase in the "ionic conductivity" and "stability" of the solid electrolyte interphase [23].

This investigation wants to delve into the feasibility of "LiRb (GeO–SiO), LiCs(GeO–SiO), NaRb(GeO–SiO), NaCs(GeO–SiO), KRb(GeO–SiO), KCs(GeO–SiO) " nanoclusters for H-storage. Therefore, it was analyzed the physico-chemical properties of mentioned heteroclusters and hydrogenated nanoclusters of "LiRb(GeO–SiO)–2H_2, LiCs(GeO–SiO)–2H_2, NaRb(GeO–SiO)–2H_2, NaCs(GeO–SiO)–2H_2, KRb(GeO–SiO)–2H_2, KCs(GeO–SiO)–2H_2".

II. Materials and Methods

Figure 1 has shown alkali metals-based nanoclusters of "LiRb (GeO–SiO), LiCs(GeO–SiO), NaRb(GeO–SiO), NaCs(GeO–SiO), KRb(GeO–SiO), KCs(GeO–SiO) " which can enhance the H-storage in cell batteries, transistors or other semiconductors. In our research, the calculations have been done by "CAM–B3LYP–D3 /EPR–3" level of theory. Fig-

ARCHIVES DES SCIENCES
A Multidisciplinary Journal

ure1 shows the process of "hydrogen adsorption" by "LiRb (GeO–SiO), LiCs(GeO–SiO), NaRb(GeO–SiO), NaCs(GeO–SiO), KRb(GeO–SiO), KCs(GeO–SiO)" nanoclusters and hydrogen-adsorbed nanoclusters of "LiRb(GeO–SiO)–2H_2, LiCs(GeO–SiO)–2H_2, NaRb(GeO–SiO)–2H_2, NaCs(GeO–SiO)–2H_2, KRb(GeO–SiO)–2H_2, KCs(GeO–SiO)–2H_2".

The "Bader charge" analysis [24] was illustrated during H-atoms grabbing by "LiRb(GeO–SiO)–2H_2, LiCs(GeO–SiO)–2H_2, NaRb(GeO–SiO)–2H_2, NaCs(GeO–SiO)–2H_2, KRb(GeO–SiO)–2H_2, KCs(GeO–SiO)–2H_2" nanoclusters (Figure 1). The rigid potential energy surface using density functional theory [25]–[27] was performed due to "Gaussian 16 revision C.01" program package [28] and "GaussView 6.1" [29]. The coordination input for hydrogen grabbing by "LiRb (GeO–SiO), LiCs(GeO–SiO), NaRb(GeO–SiO), NaCs(GeO–SiO), KRb(GeO–SiO), KCs(GeO–SiO)" has been calculated using "LANL2DZ" and "6-311+G (d,p)" basis sets.

III. Results and Discussion

A. TDOS analysis

In "isolated system (such as molecule) ", the energy levels are discrete, the concept of "density of state (DOS)" is supposed to be completely valueless in this situation. Therefore, the "original total DOS (TDOS)" of isolated system can be written as [30]:

$$TDOS\ (E) = \sum_i \delta\,(E - \epsilon_i\,). \tag{1}$$

The normalized "Gaussian function" is defined as:

$$G\,(x) = \frac{1}{c\sqrt{2\pi}} e^{-\frac{x^2}{2c^2}}, \quad \text{where} \quad c = \frac{\mathrm{FWHM}}{2\sqrt{2\ln x}}. \tag{2}$$

"FWHM (full width at half maximum)" is an adjustable parameter in "Multiwfn". In the "TDOS map", each discrete vertical line corresponds to a "molecular orbital (MO)", the dashed line highlights the position of "HOMO". The curve is the "TDOS" simulated based on the distribution of "MO" energy levels.

Regarding adsorption behavior of hydrogen by "LiRb(GeO–SiO), LiCs(GeO–SiO), NaRb(GeO–SiO), NaCs(GeO–SiO), KRb(GeO–SiO), KCs(GeO–SiO)" nanoclusters, "TDOS" has been measured. This parameter can indicate the existence of important chemical interactions often on the "convex side" (Figure 2 a,a′, b,b′, c,c′, d,d′, e,e′, f,f′).

During formation of "LiRb (GeO–SiO), LiCs(GeO–SiO), NaRb(GeO–SiO), NaCs(GeO–SiO), KRb(GeO–SiO) " (Figure 2 a,b,c,d,e) and hydrogenated nanoclusters containing "LiRb(GeO–SiO)–2H_2, LiCs(GeO–SiO)–2H_2, NaRb(GeO–SiO)–2H_2, NaCs(GeO–SiO)–2H_2" (Fig.2a′,b′,c′,d′,e′) have shown the steepest peaks around "–0.3, –0.45 and –0.60 a.u." due to covalent bond between two atoms of "Li/Rb, Li/Cs, Na/Rb, Na/Cs" with (GeO–SiO) nanocluster.

However, the "TDOS" curve for KRb (GeO–SiO) and KRb (GeO–SiO)–2H_2 nanoclusters have shown four pointed peaks around "–0.3, –0.45, –0.60, –0.75 a.u." due to covalent bond between atoms of K, Rb, Cs with (GeO–SiO) nanocluster through hydrogen storage with maximum density of state of ≈ 24 around –0.30 a.u. (Figure 2 f,f′).

B. LOL analysis

"Localized orbital locator (LOL)" has a similar expression compared to "electron localization function (ELF)" [31].

$$\mathrm{LOL}(\mathbf{r}) = \frac{\tau\,(\mathbf{r})}{1+\tau\,(\mathbf{r})}; \tau\,(\mathbf{r}) = \frac{D_0\,(\mathbf{r})}{\frac{1}{2}\,\sum_i \eta_i |\nabla\varphi_i\,(\mathbf{r})|^2}, \tag{3}$$

$$D_0\,(\mathrm{r}) = \frac{3}{10}\left(6\pi^2\right)^{2/3}\left[\rho_\alpha\,(\mathrm{r})^{5/3} + \rho_\beta\,(\mathrm{r})^{5/3}\right]. \tag{4}$$

"Multiwfn" [32], [33] also supports the approximate version of "LOL" defined by "Tsirelson and Stash" [34], namely the actual kinetic energy term in "LOL" is replaced by "second-order gradient expansion like ELF" which may demonstrate a broad span of bonding samples. This "Tsirelson's version of LOL" can be activated by setting "ELFLOL_type to 1. For special reason", if "ELFLOL_type in settings.ini is changed from 0 to 2", another formalism will be used:

$$\mathrm{LOL}(\mathbf{r}) = \frac{1}{1+\ [1/\tau\,(\mathbf{r})]^2}. \tag{5}$$

If the parameter "ELFLOL_cut in settings.ini is set to x", then "LOL will be zero where LOL is less than x".

Trapping of hydrogens by "LiRb (GeO–SiO), LiCs(GeO–SiO), NaRb(GeO–SiO), NaCs(GeO–SiO), KRb(GeO–SiO), KCs(GeO–SiO)" (Figure 3 a,b,c,d,e,f).nanoclusters towards formation of "LiRb(GeO–SiO)–2H_2, LiCs(GeO–SiO)–2H_2, NaRb(GeO–SiO)–2H_2, NaCs(GeO–SiO)–2H_2, KRb(GeO–SiO)–2H_2, KCs(GeO–SiO)–2H_2" might be described by "LOL graphs" due to achieving their "delocalization/localization" characterizations of electrons and chemical bonds (Figure 3 a′,b′,c′,d′,e′,f′).

An isosurface map has shown the electron delocalization in "LiRb (GeO–SiO) (Figure 3 a), LiRb(GeO–SiO)–2H_2 (Figure 3 a′), LiCs (GeO–SiO) (Figure 3 b), LiCs(GeO–SiO)–2H_2 (Figure 3 b′), NaRb (GeO–SiO) (Figure 3 c), NaRb(GeO–SiO)–2H_2 (Figure 3 c′), NaCs (GeO–SiO) (Figure 3 d), NaCs(GeO–SiO)–2H_2 (Figure 3 d′), KRb (GeO–SiO) (Fig.4e), KRb(GeO–SiO)–2H_2 (Figure 3 e′), KCs (GeO–SiO) (Figure 3 f),and KCs(GeO–SiO)–2H_2" (Figure 3 f′) through labeling atoms of "O10, O12, Si13, O24, O26, Ge28, X31(X=Li, Na or K), Y32 (Y=Rb or Cs) and H33, H34, H35, H36". In fact, the "counter map of LOL" can confirm that LiRb (GeO–SiO), LiCs(GeO–SiO), NaRb(GeO–SiO), NaCs(GeO–SiO), KRb(GeO–SiO), KCs(GeO–SiO) nanoclusters may increase the efficiency during hydrogen adsorption towards formation of LiRb(GeO–SiO)–2H_2, LiCs(GeO–SiO)–2H_2, NaRb(GeO–SiO)–2H_2, NaCs(GeO–SiO)–2H_2, KRb(GeO–SiO)–2H_2, KCs(GeO–SiO)–2H_2.

Besides, "intermolecular orbital overlap integral" is important in discussions of intermolecular charge transfer which can calculate "HOMO-HOMO" and "LUMO-LUMO" overlap integrals between the H_2 molecules and heteroclusters of LiRb(GeO–SiO), LiRb(GeO–SiO)–2H_2, LiCs(GeO–SiO),

LiCs(GeO–SiO)–2H_2, NaRb(GeO–SiO), NaRb(GeO–SiO) –2H_2, NaCs(GeO–SiO), NaCs(GeO–SiO)–2H_2, KRb(GeO–SiO), KRb(GeO–SiO)–2H_2, KCs(GeO–SiO), and KCs(GeO–SiO)–2H_2 nanoclusters. The applied wavefunction level is "CAM–B3LYP–D3/6–311+G (d, p)" that corresponds to "HOMO and LUMO" (Table1). The layered germanium-silicon oxide improved by alkali metal lithium doping have indicated the structural stability of lithium-, sodium- or potassium-ion batteries through the reported stability energy in Table1. A small portion of Rb or Cs entered the Ge–Si layer to replace the Li, Na or K sites might improve the structural stability of the electrode material at high multiplicity, thereby improving the capacity retention rate.

In summary, the addition of "Rb or Cs" ions into electrolyte greatly improves the cycling performance of the hard carbon anode in "lithium-, sodium-, or potassium-ion" batteries. This improvement is attributed to the participation of the "Rb or Cs" ions to form a highly conductive, which results in a lower cell reaction resistance. Therefore, the battery cells with "Rb or Cs" ions as the additive have not only higher specific capacity and smaller polarization, but also more stable.

IV. Conclusions

H-capture by the nanoclusters of "LiRb (GeO–SiO), LiCs(GeO–SiO), NaRb(GeO–SiO), NaCs(GeO–SiO), KRb(GeO–SiO), KCs(GeO–SiO)" was investigated by "first-principles computations of DFT method". The changes of charge density defined a notable charge transfer in "LiRb (GeO–SiO), LiCs(GeO–SiO), NaRb(GeO–SiO), NaCs(GeO–SiO), KRb(GeO–SiO), KCs(GeO–SiO)". The fluctuation in charge density values describes that the electronic densities were in the boundary of "adsorbate/adsorbent" atoms during the adsorption status. Besides, thermodynamic parameters describing H-grabbing by alkali metals-based nanoclusters of "LiRb (GeO–SiO), LiCs(GeO–SiO), NaRb(GeO–SiO), NaCs(GeO–SiO), KRb(GeO–SiO), KCs(GeO–SiO)" have been studied consisting of internal process of the "adsorbent–adsorbate" system.

It is well established that the addition of Li, Na or K to cell batteries may increase the energy storage in cell batteries. In this work, we explore the effect of "Rb- or Cs-doped lithium-, sodium-or potassium-ion" batteries. Moreover, "hydrogen bond (H-bond)" accepting sites by "LiRb (GeO–SiO), LiCs(GeO–SiO), NaRb(GeO–SiO), NaCs(GeO–SiO), KRb(GeO–SiO), KCs(GeO–SiO) " can alleviate "parasitic hydrogen evolution" in aqueous electrolytes in lithium, sodium, or potassium-ion batteries. The results of this work show that a addition in the form of "XY(GeO–SiO) (X = Li,Na,K/Y=Rb,Cs) " can increase the capacity battery cell.

References

[1] Yang, H., & Wu, N. (2022). Ionic conductivity and ion transport mechanisms of solid-state lithium-ion battery electrolytes: A review. *Energy Science & Engineering, 10*(5), 1643-1671.

[2] Walvekar, H., Beltran, H., Sripad, S., & Pecht, M. (2022). Implications of the electric vehicle manufacturers' decision to mass adopt lithium-iron phosphate batteries. *Ieee Access, 10*, 63834-63843.

[3] Choi, D., Shamim, N., Crawford, A., Huang, Q., Vartanian, C. K., Viswanathan, V. V., ... & Sprenkle, V. L. (2021). Li-ion battery technology for grid application. *Journal of Power Sources, 511*, 230419.

[4] Ahmad, T., & Zhang, D. (2020). A critical review of comparative global historical energy consumption and future demand: The story told so far. *Energy Reports, 6,* 1973-1991.

[5] Mlilo, N., Brown, J., & Ahfock, T. (2021). Impact of intermittent renewable energy generation penetration on the power system networks–A review. *Technology and Economics of Smart Grids and Sustainable Energy, 6*(1), 1-19.

[6] Rautela, R., Yadav, B. R., & Kumar, S. (2023). A review on technologies for recovery of metals from waste lithium-ion batteries. *Journal of Power Sources, 580*, 233428.

[7] Tan, A. K., & Paul, S. (2024). Beyond Lithium: Future Battery Technologies for Sustainable Energy Storage. *Energies, 17*(22), 5768.

[8] Singh, A. N., Islam, M., Meena, A., Faizan, M., Han, D., Bathula, C., ... & Nam, K. W. (2023). Unleashing the potential of sodium-ion batteries: current state and future directions for sustainable energy storage. *Advanced Functional Materials, 33*(46), 2304617.

[9] Gu, Z. Y., Guo, J. Z., Cao, J. M., Wang, X. T., Zhao, X. X., Zheng, X. Y., ... & Wu, X. L. (2022). An advanced high-entropy fluorophosphate cathode for sodium-ion batteries with increased working voltage and energy density. *Advanced Materials, 34*(14), 2110108.

[10] Jin, Y., Le, P. M., Gao, P., Xu, Y., Xiao, B., Engelhard, M. H., ... & Zhang, J. G. (2022). Low-solvation electrolytes for high-voltage sodium-ion batteries. *Nature Energy, 7*(8), 718-725.

[11] Zhang, X., Xiong, T., He, B., Feng, S., Wang, X., Wei, L., & Mai, L. (2022). Recent advances and perspectives in aqueous potassium-ion batteries. *Energy & Environmental Science, 15*(9), 3750-3774.

[12] Ge, J., Fan, L., Rao, A. M., Zhou, J., & Lu, B. (2022). Surface-substituted Prussian blue analogue cathode for sustainable potassium-ion batteries. *Nature Sustainability, 5*(3), 225-234.

[13] Ji, B., Yao, W., Zheng, Y., Kidkhunthod, P., Zhou, X., Tunmee, S., ... & Tang, Y. (2020). A fluoroxalate cathode material for potassium-ion batteries with ultra-long cyclability. *Nature Communications, 11*(1), 1225.

[14] Nazeer, W., Farooq, A., Younas, M., Munir, M., & Kang, S. M. (2018). On molecular descriptors of carbon nanocones. *Biomolecules, 8*(3), 92.

[15] Zhao, J., Li, Z., Cole, M. T., Wang, A., Guo, X., Liu, X., ... & Dai, Q. (2021). Nanocone-shaped carbon nanotubes field-emitter array fabricated by laser ablation. *Nanomaterials, 11*(12), 3244.

[16] Rong, Y., Cao, Y., Guo, N., Li, Y., Jia, W., & Jia, D. (2016). A simple method to synthesize V2O5 nanostructures with controllable morphology for high performance Li-ion batteries. *Electrochimica Acta, 222*, 1691-1699.

[17] Yodsin, N., Sakagami, H., Udagawa, T., Ishimoto, T., Jungsuttiwong, S., & Tachikawa, M. (2021). Metal-doped carbon nanocones as highly efficient catalysts for hydrogen storage: Nuclear quantum effect on hydrogen spillover mechanism. *Molecular Catalysis, 504*, 111486.

[18] Taha, H. O., El Mahdy, A. M., El Shemy, F. E. S., & Hassan, M. M. (2023). Hydrogen storage in SiC, GeC, and SnC nanocones functionalized with nickel, Density Functional Theory—Study. *International Journal of Quantum Chemistry, 123*(3), e27023.

[19] Wei, T., Zhou, Y., Sun, C., Guo, X., Xu, S., Chen, D., & Tang, Y. (2024). An intermittent lithium deposition model based on CuMn-bimetallic MOF derivatives for composite lithium anode with ultrahigh areal capacity and current densities. *Nano Research, 17*(4), 2763-2769.

[20] Mollaamin, F., & Monajjemi, M. (2024). Nanomaterials for sustainable energy in hydrogen-fuel cell: Functionalization and characterization of carbon nano-semiconductors with silicon, germanium, tin or lead through density functional theory study. *Russian Journal of Physical Chemistry B, 18*(2), 607-623.

[21] Mollaamin, F., Shahriari, S., & Monajjemi, M. (2024). Influence of transition metals for emergence of energy storage in fuel cells through hydrogen adsorption on the MgAl surface. *Russian Journal of Physical Chemistry B, 18*(2), 398-418.

[22] Mollaamin, F. (2024). Competitive intracellular hydrogen-nanocarrier among aluminum, carbon, or silicon implantation: a novel technology of eco-friendly energy storage using research density functional theory. *Russian Journal of Physical Chemistry B, 18*(3), 805-820.

[23] Che, H., Liu, J., Wang, H., Wang, X., Zhang, S. S., Liao, X. Z., & Ma, Z. F. (2017). Rubidium and cesium ions as electrolyte additive for improving

ARCHIVES DES SCIENCES
A Multidisciplinary Journal

Heteroclusters	$E_s \times 10^{-3}$ (kcal/mol)	Dipole moment (debye)	E_{HOMO} (eV)	E_{LUMO} (eV)	$\Delta E = E_{LUMO} - E_{HOMO}$ (eV)
LiRb (GeO–SiO)	-986.6092	1.1509	-6.0501	-5.0314	1.0187
LiRb(GeO–SiO)–$2H_2$	-988.0376	1.7979	-6.0318	-5.0177	1.0140
LiCs(GeO–SiO)	-983.9461	1.0986	-5.8000	-5.0456	0.7544
LiCs(GeO–SiO)–$2H_2$	-985.3503	1.3745	-5.7932	-5.0205	0.7727
NaRb(GeO–SiO)	-982.0238	1.3744	-6.0241	-5.0119	1.0112
NaRb(GeO–SiO)–$2H_2$	-983.4472	1.8613	-6.0161	-5.0091	1.0069
NaCs(GeO–SiO)	-979.3589	0.9598	-5.7525	-5.0603	0.6921
NaCs(GeO–SiO)–$2H_2$	-980.7597	1.3015	-5.7777	-5.0073	0.7703
KRb(GeO–SiO)	-999.5136	1.5095	-6.0063	-5.0020	1.0044
KRb(GeSiO)–$2H_2$	-1000.9243	1.7183	-6.0122	-5.0133	1.0000
KCs(GeSiO)	-996.8456	0.5364	-5.8088	-5.3009	0.5080
KCs(GeO–SiO)–$2H_2$	-998.2354	0.9823	-5.7579	-5.0392	0.7187

Table 1: "Stability energy (kcal/mol), dipole moment (debye), LUMO (eV), HOMO(eV), and energy gap (ΔE) (eV)" for LiRb (GeO–SiO), LiCs(GeO–SiO), NaRb(GeO–SiO), NaCs(GeO–SiO), KRb(GeO–SiO), KCs(GeO–SiO) through hydrogen grabbing and formation of LiRb(GeO–SiO)–$2H_2$, LiCs(GeO–SiO)–$2H_2$, NaRb(GeO–SiO)–$2H_2$, NaCs(GeO–SiO)–$2H_2$, KRb(GeO–SiO)–$2H_2$, KCs(GeO–SiO)–$2H_2$ heteroclusters

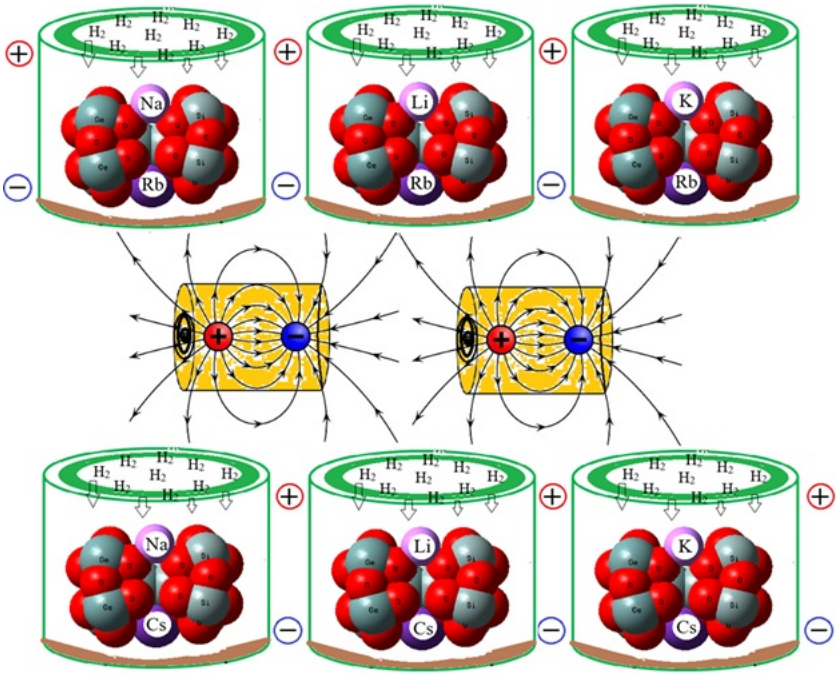

Figure 1: Adding "Li, Na, K" to (GeO–SiO) nanoclusters accompanying Rb or Cs doping and formation of LiRb (GeO–SiO), LiCs(GeO–SiO), NaRb(GeO–SiO), NaCs(GeO–SiO), KRb(GeO–SiO), KCs(GeO–SiO) nanoclusters towards energy storage through hydrogen adsorption as LiRb(GeO–SiO)–$2H_2$, LiCs(GeO–SiO)–$2H_2$, NaRb(GeO–SiO)–$2H_2$, NaCs(GeO–SiO)–$2H_2$, KRb(GeO–SiO)–$2H_2$, KCs(GeO–SiO)–$2H_2$ in novel batteries

performance of hard carbon anode in sodium-ion battery. *Electrochemistry Communications, 83*, 20-23.

[24] Henkelman, G., Arnaldsson, A., & Jónsson, H. (2006). A fast and robust algorithm for Bader decomposition of charge density. *Computational Materials Science, 36*(3), 354-360.

[25] Mollaamin, F., & Monajjemi, M. (2024). Adsorption ability of Ga5N10 nanomaterial for removing metal ions contamination from drinking water by DFT. *International Journal of Quantum Chemistry, 124*(2), e27348.

[26] Mollaamin, F., & Monajjemi, M. (2023). Molecular modelling framework of metal-organic clusters for conserving surfaces: Langmuir sorption through the TD-DFT/ONIOM approach. *Molecular Simulation, 49*(4), 365-376.

[27] Vosko, S. H., Wilk, L., & Nusair, M. (1980). Accurate spin-dependent electron liquid correlation energies for local spin density calculations: a critical analysis. *Canadian Journal of physics, 58*(8), 1200-1211.

[28] Frisch, M. E., Trucks, G. W., Schlegel, H. B., Scuseria, G. E., Robb, M., Cheeseman, J. R., ... & Fox, D. J. (2016). *Gaussian 16*.

[29] Dennington, R. D. I. I., Keith, T. A., & Millam, J. M. (2016). GaussView, version 6.0. 16. *Semichem Inc Shawnee Mission KS, 13*(1).

[30] Becke, A. D., & Edgecombe, K. E. (1990). A simple measure of electron localization in atomic and molecular systems. *The Journal of Chemical Physics, 92*(9), 5397-5403.

[31] Schmider, H. L., & Becke, A. D. (2000). Chemical content of the kinetic energy density. *Journal of molecular structure: THEOCHEM, 527*(1-3), 51-61.

[32] Lu, T., & Chen, F. (2012). Multiwfn: A multifunctional wavefunction analyzer. *Journal of Computational Chemistry, 33*(5), 580-592.

[33] Lu, T. (2024). A comprehensive electron wavefunction analysis toolbox for chemists, Multiwfn. *The Journal of Chemical Physics, 161*(8), 082503.

[34] Tsirelson, V. G., & Stash, A. (2002). Analyzing experimental electron density with the localized-orbital locator. *Structural Science, 58*(5), 780-785.

ARCHIVES DES SCIENCES
A Multidisciplinary Journal

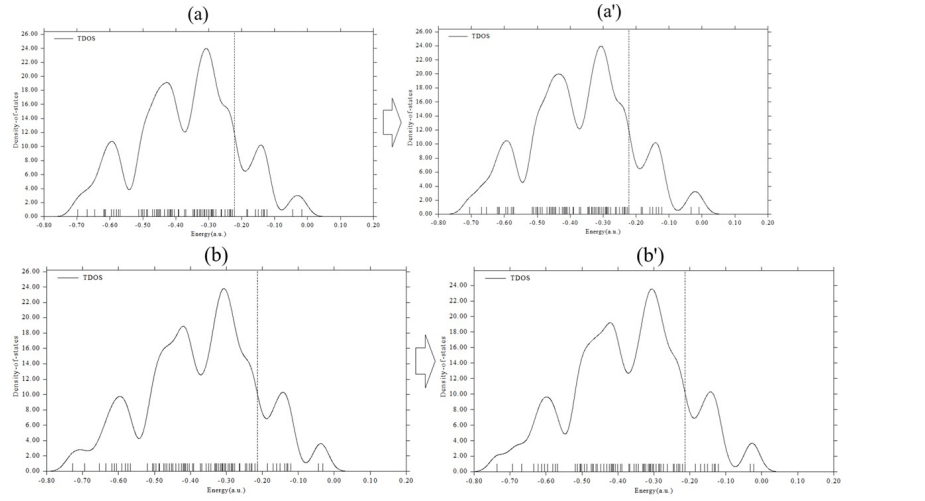

(a) a,a′,b,b′

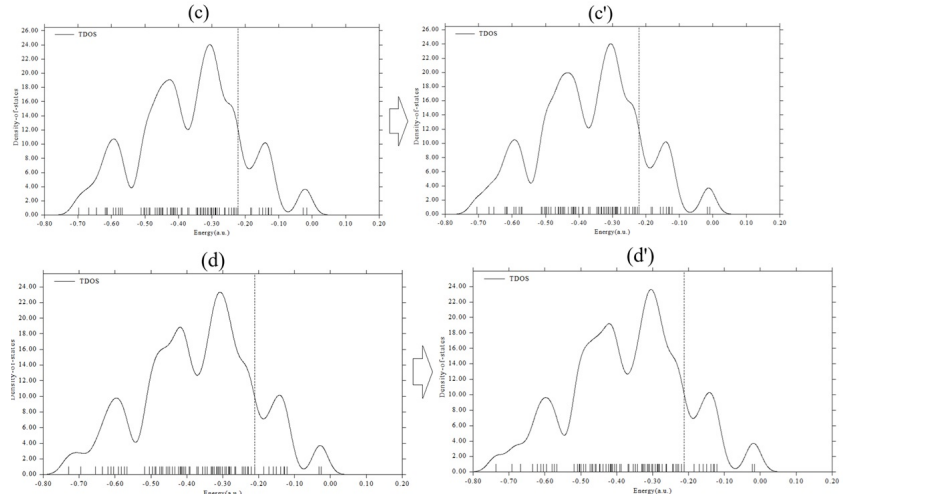

(b) c,c′,d,d′

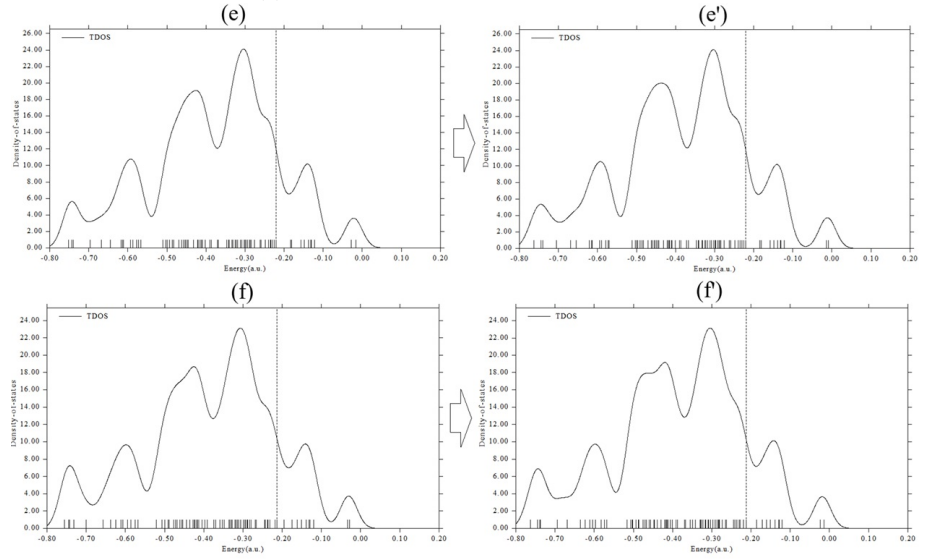

(c) e,e′,f,f′

Figure 2: "TDOS graphs" of (a) LiRb (GeO–SiO), (a′) LiRb(GeO–SiO)–$2H_2$, (b) LiCs(GeO–SiO), (b′) LiCs(GeO–SiO)–$2H_2$, (c) NaRb(GeO–SiO), (c′) NaRb(GeO–SiO)–$2H_2$, (d) NaCs(GeO–SiO), (d′) NaRb(GeO–SiO)–2H2, (e) KRb(GeO–SiO), (e′) KRb(GeO–SiO)–$2H_2$, (f) KCs(GeO–SiO), (f′) KCs(GeO–SiO)–$2H_2$ nanoclusters.

ARCHIVES DES SCIENCES
A Multidisciplinary Journal

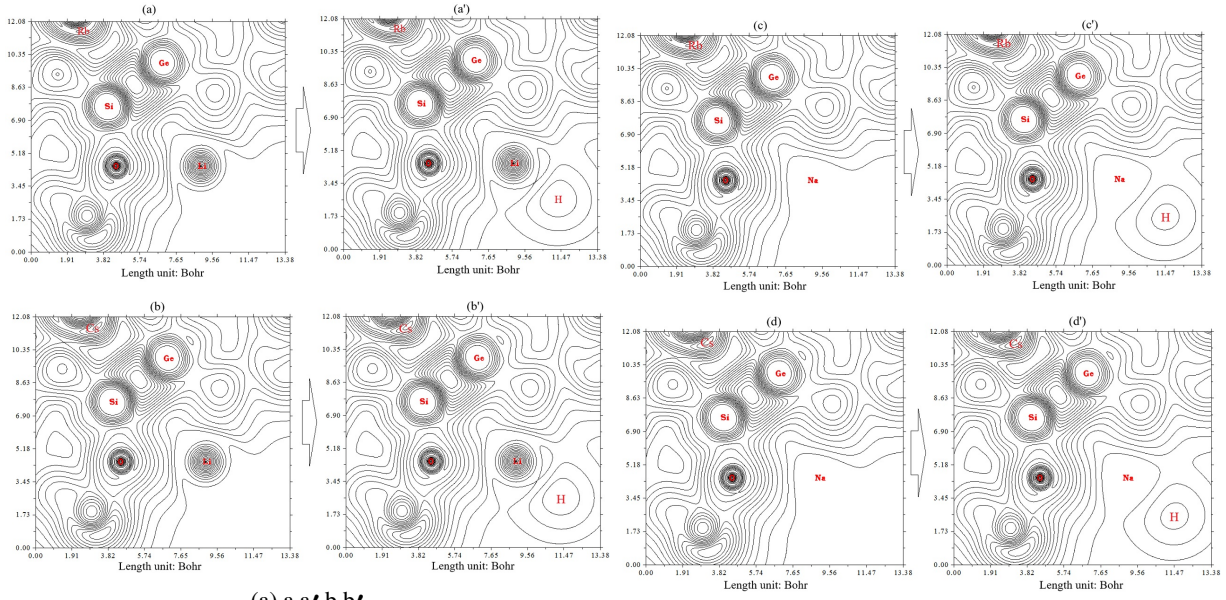

(a) a,a′,b,b′

(b) c,c′,d,d′

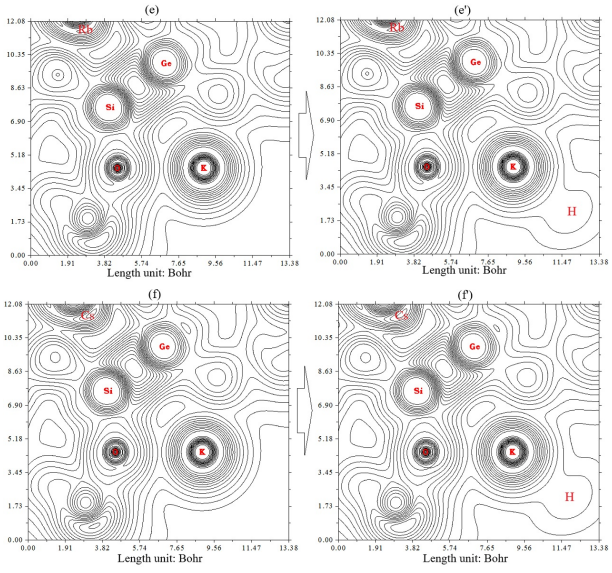

(c) e,e′,f,f′

Figure 3: The "counter map of LOL graphs" for (a) LiRb (GeO–SiO), (a′) LiRb(GeO–SiO)–2H_2, (b) LiCs(GeO–SiO), (b′) LiCs(GeO–SiO)–2H_2, (c) NaRb(GeO–SiO), (c′) NaRb(GeO–SiO)–2H_2, (d) NaCs(GeO–SiO), (d′) NaRb(GeO–SiO)–2H2, (e) KRb(GeO–SiO), (e′) KRb(GeO–SiO)–2H_2, (f) KCs(GeO–SiO), (f′) KCs(GeO–SiO)–2H_2 nanoclusters